13th ewtec 2019
Proceedings of the 13th European Wave and Tidal Energy Conference 1-6 Sept 2019, Naples, Italy

CFD surface effects on flow conditions and tidal stream turbine performance

Catherine Lloyd, Matthew Allmark, Robert Ellis, Stephanie Ordonez, Allan Mason-Jones, Cameron Johnstone, Tim O'Doherty, Gregory Germain and Benoit Gaurier

Abstract— **This study presents a comparison of the turbine performance estimated by numerical models with 2 different surface boundary conditions; namely a 'free surface' and a 'free slip' surface condition. Validation of the models was carried out using experimental data from testing at the French Research Institute for Exploitation of the Sea (IFREMER). The average thrust and torque results were compared, as well as the fluctuation in the loadings between the numerical models. It was found that differences existed between the 2 models, in particular for the prediction of the average thrust on the hub as well as the magnitude of fluctuation in the torque for an individual blade. Therefore, this study has shown that it could be necessary to use the more complex and time consuming 'free surface' model if the transient loadings on the blades are of interest. If only the total average loading is of interest, then the 'free slip' model would be adequate.**

Keywords - **ANSYS CFX, Computational Fluid Dynamics, Free Surface, Marine Energy, Tidal Stream Turbine.**

I. Introduction

With solar photovoltaic and wind energy technologies being largely developed [1], the oceans represent a huge resource which is yet to be fully utilised. Tidal currents are a predictable source of renewable energy with the advancement of Horizontal Axis Tidal Turbines (HATT) being the most developed technology in the tidal stream sector. It is predicted by [2], that deployment of 3.4 TW of wave and tidal energy capacity could be present by 2050, with 350 TWh/year present in Europe.

Complex flow conditions are what makes deployment and survival of tidal energy devices a challenge for Tidal Stream Turbine (TST) manufacturers. Laboratory experiments can be carried out to reproduce realistic ocean flow conditions. However, with advances in technology and quicker processing times, Computational Fluid Dynamics (CFD) has become a widely adopted tool to investigate the loadings and performance of tidal devices in various flow conditions.

Numerical models can be produced in a variety of ways using many different CFD packages. The representation of the turbine can be achieved in predominantly 4 ways: the Actuator Disc Method (ADM), the Actuator Line Model (ALM), the Virtual Blade Model (VBM) and the Moving Reference Frame (MRF) technique. The ADM comprises of a disc region, the same area as the turbine, where forces are applied to the flow as they would be imposed by a turbine. Computationally, this method is much less expensive than a 'fully resolved' model, however, simulations are usually steady state and therefore lead to time averaged results. Therefore, this method is mainly applied to models investigating large-scale flow effects, such as the study by [3], simulating multi-turbine arrays. The ALM consists of actuator lines which represent each turbine blade. These are divided into a number of equally spaced segments whereby the body forces are imposed on the flow, equal and opposite to the lift and drag forces experienced by the turbine. This method is used by [4] for multiple turbines and array simulations, while [5] uses the model to investigate support structure influence on contra rotating rotors. As stated by [5], the ADM cannot capture fluctuations in power output due to blade-structure interaction due to the use of a disc to represent the turbine, therefore the ALM better for examining these transient features. The VBM was used by [6] to simulate a HATT using ANSYS FLUENT. In this method the blades are 'virtual', and representation of the turbine is achieved by adding body forces in the x, y and z directions. This method has limitations, whereby the lift and drag forces are averaged over a full rotation of the turbine and so don't account for transient flow characteristics. The 'fully resolved' model is achieved using the MRF technique with a sliding mesh between the rotating 'turbine' domain and the stationary 'fluid' domain. This method accounts for the transient interaction effects across the domain interface. Numerical modelling using the MRF technique has been investigated by [7] and [8] using a 0.5m and 10m turbine respectively. Both studies found that the numerical turbine performance characteristics displayed good agreement with the comparable experimental data.

As well as having multiple methods for modelling the turbine, the upper boundary surface effects can also be represented in different ways. A 'free slip wall' boundary condition could be implemented which gives the velocity

ID number: 1303. Conference track: Tidal hydrodynamic modelling.

The authors acknowledge support from SuperGen UK Centre for Marine Energy (EPSRC: EP/N020782/1) and Cardiff University for providing funding. C. Lloyd, M. Allmark, R. Ellis, A. Mason-Jones and T. O'Doherty are all with Cardiff Marine Energy Research Group in the School of Engineering at Cardiff University, Queens Buildings, Cardiff, CF24 3AA, UK (email: LloydC11@cardiff.ac.uk).

S. Ordonez and C. Johnstone are with the Energy Systems research Unit in the University of Strathclyde, Glasgow, G1 1XJ, UK.

G. Germain and B. Gaurier are with IFREMER, Centre Manche, Mer du Nord – 150, Quai Gambetta – 62200, Boulogne-sur-Mer.

component of the water parallel to the boundary a finite value. Alternatively, a 'free surface' model could be generated using a 2-fluid multiphase approach with a distinct interface between the 2 phases.

The 'free slip' upper surface condition has been widely used to compare average turbine performance characteristics to experimental data. As shown by [6], ANSYS FLUENT was used to create a 'free slip' simulation to investigate the numerical predictions of average power and torque generated by a 0.5m diameter HATT. A comparative study was found to provide excellent agreement between both data sets. Further development of this work was carried out by [7], to investigate the effect of flow directionality on turbine performance, and again found that the average CFD and experimental results were in good agreement. Similar results were found by [9] when making comparisons between numerical and experimental data using a 0.8m diameter turbine. Average results for the power coefficient (C_p) and thrust coefficient (C_t) in both sets of results were found to give good agreement. These studies were all carried out in uniform flow conditions and made comparisons between time averaged performance characteristics.

A 'free surface' model was developed by [10] using the 'level set' method to track the air-water interface. A sliding interface was used to provide a fully resolved model using a 3 bladed turbine with a diameter of 0.8m. These simulations were able to capture the effect of the free surface on the hydro-dynamic loading of the rotor. Further testing was carried out using airy wave conditions showing that more complex flow conditions were possible using this type of model. a numerical model using An in-house code, 'CgLes' [11], developed by [12] implemented 2 different free surface schemes, the 'height function' method and the 'level set' method. It was noted that existence of the free surface, in comparison to the 'free slip' approximation, caused a slight increase in the Cp, predicting that locating the turbine closer to the free surface or in the presence of surface waves, this could increase even more. ANSYS FLUENT was used by [13] to implement the Volume of Fluid (VOF) method in order to create a 'free surface' numerical model. The effect of varying turbine thrust on the 'free surface' was investigated and it was found that the extraction of energy from tidal currents resulted in a 'free surface' drop behind the turbine which are not seen in a 'free slip' arrangement of the model.

Analysis of previous literature shows that both types of model can accurately replicate average experimental performance results for a single TST in uniform flow. The 'free surface' model can be much more computationally expensive than the 'free slip' model due to the refined mesh requirements around the 'free surface' interface. Therefore, the complexities of the 2 different model types are examined as well as identifying the differences between the time averaged and transient results.

This paper presents a study of 2 different types of model setup – the 'free slip' and the 'free surface' model – developed using ANSYS CFX 18.0. Comparisons are made against experimental data obtained by Cardiff and Strathclyde Universities at the French Research Institute for Exploitation of the Sea (IFREMER). The flow conditions generated by each model as well as the average and transient turbine performance characteristics were examined.

NOMENCLATURE.

Symbol	Quantity	Unit
A	Swept Area	m²
C_p	Power coefficient	[ ]
C_q	Torque coefficient	[ ]
C_t	Thrust coefficient	[ ]
D	Turbine Diameter	m
F	Thrust	N
P	Power	W
P_{ref}	Reference pressure	Pa
P_{rel}	Relative pressure	Pa
Q	Torque	Nm
R	Radius	m
V	Overall volume	m³
V_x	Volume occupied by fluid x	m³
W	Streamwise velocity	m/s
g	Gravitational acceleration	m/s²
h	Water depth	m
r	Local radius	m
r_1	Volume fraction of fluid x	[ ]
Δt	Time step	s
y	Vertical distance from free surface level	m
λ	Tip speed ratio	[ ]
ω	Angular velocity	rad/s
θ	Angle	°
ρ	Density	kg/m³

II. EXPERIMENTAL TESTING

A) Model tidal stream turbine

The TST used in this experimental testing was designed by Cardiff Marine Energy Research Group (CMERG). The model scale turbine - approximately 1:20 scale - is a 3 bladed, 0.9m diameter, Horizontal Axis Tidal Turbine (HATT), as shown in Figure 1a. The blade design was based upon the Wortmann FX63-137 aerofoil, as detailed by [14], while the turbine design and manufacture was carried out as detailed by [15]. An optimum pitch angle of

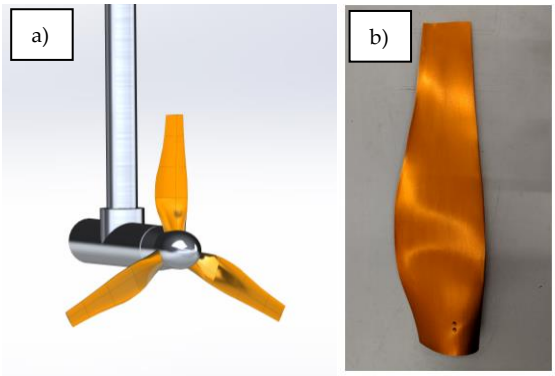

Figure 1. Diagram of: (a) the full turbine and; (b) the new blade design.

TABLE I.
BLADE COMPOSITION DETAILS.

r/R	Blade Chord (mm)
0.146	72.5
0.229	87.8
0.305	103.1
0.382	1.906
0.459	109.5
0.536	105.1
0.615	93.1
0.692	83.6
0.768	73.6
0.845	67.6
0.922	62.8
1.0	58.9

TABLE II.
MAIN TURBINE CHARACTERISTICS SUMMARY.

Characteristic	Description	Units
No. Blades	3	[ ]
Blade length	384.5	mm
Pitch angle	8	°
Twist distribution	19	°
Turbine diameter	900	mm
Hub diameter	130	mm

8° was used while the blades had a 19° twist distribution as shown in Figure 1b. Table I shows the blade composition while Table II shows a summary of the main turbine characteristics.

B) Wave-current flume tank

Experimental testing was carried out at IFREMER, Boulogne-Sur-Mer, France. The dimensions of the flume tank are 4m wide, 2m deep and 18m long with a general flow turbulence of ≈3% [16].

C) Experimental setup

The turbine was installed at a depth of 1m giving a clearance, in still water, of 0.61D. The blockage ratio for the flume tank was 7.95% which was low enough not to interfere with the flow [17]. All testing was conducted using speed control, whereby the angular velocity of the turbine was controlled so that it remained constant. The experiments were carried out at an average flow velocity of ≈ 1 m/s and measurements for each test were taken for at least 100 seconds. Laser Doppler Velocimetry (LDV) was used to measure the flow velocity in the streamwise and vertical directions at multiple points through the water depth. This was carried out to establish whether the flow was uniform or if it had a sheared profile. The turbine was fully instrumented, as detailed in [15], which meant the angular velocity, torque and thrust could be measured and then compared to numerical models developed using CFD. Figure 2 shows the turbine being tested with the LDV upstream at IFREMER.

III. NUMERICAL METHODOLOGY

The numerical models were developed to replicate the experimental testing facilities of IFREMER. This enabled direct comparison between the experimental data and the numerical model results. A 'free surface' and a 'free slip' numerical model were created to explore the differences between each model set up and their accuracy when compared to model scale experimental results. The model development has been split up into 3 main sections: A*) Geometry*, *B) Mesh* and *C) Physics Setup*.

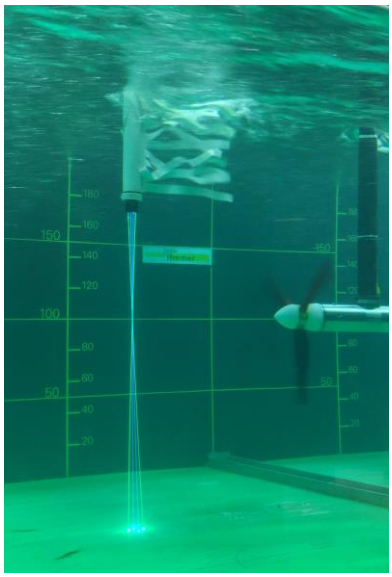

Figure 2. Experimental setup at IFREMER.

A) Geometry

The turbine geometry was developed in Solidworks 2016 and then imported into ANSYS ICEM 18.0 [18] where the overall geometry was assembled and the mesh generation was carried out. The coordinate frame was set with the positive z-axis in the streamwise direction, y-axis in the vertical direction and x-axis perpendicular to the YZ plane as shown in Figure 3.

The numerical domain dimensions were different to that of the experimental facilities due to computational requirements. The width remained the same at 4m, but the height of the domain was modified depending on the boundary condition used for the upper surface. The 'free surface' model required space for both water and air in the overall domain and so an air space of 0.86m was added above the 2m water depth giving an overall height of 2.86m. The 'free slip' model was single fluid flow only and therefore the height of the domain was the same as the depth of the water (2m). A computational domain length of 20m was used to generate the desired flow conditions in a known region of the model domain.

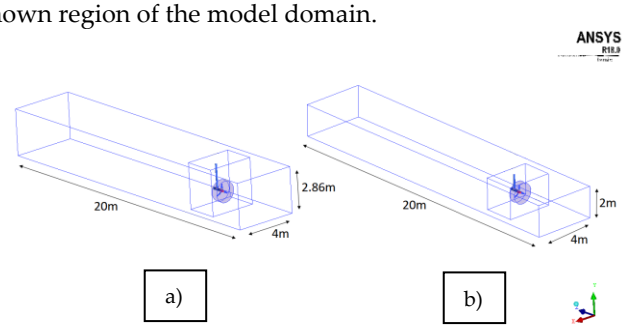

Figure 3. Geometry development for: (a) 'free surface' and; (b) 'free slip' model.

The rotating part of the turbine was enclosed in a cylindrical region to create 2 separate domains within the model. This allowed the rotating Multiple Frames of Reference (MFR) technique to be used which allows a domain to rotate around a given axis at a specified angular velocity, simulating the turbine rotation. This method allows a stationary (flume tank) and rotating (turbine) domain to interact using a sliding interface and is detailed further in section C). The diameter of the MFR cylinder was 1.3m, as recommended by [14], as it was found that a smaller diameter would influence the turbine results yet a bigger diameter had no effect.

B) Mesh

The domain was split into 3 sections to ease the process of mesh generation. Section 1 contained the MFR cylinder enclosing the turbine, section 2 encompassed the whole turbine and support structure, while section 3 included the rest of the flume tank, as shown in Figure 4.

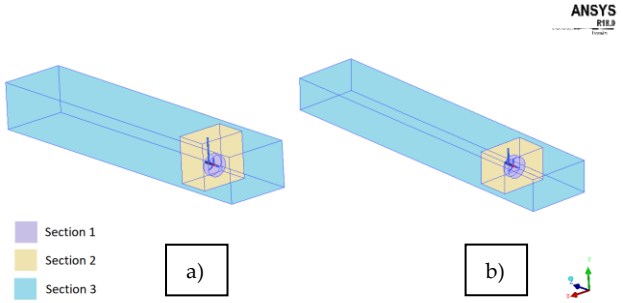

Figure 4. Different mesh sections for: (a) 'free surface' and; (b) 'free slip' models.

The mesh was generated using a mixture of 'hexa' and 'tetra' meshing. The 'hexa' mesh was developed using a 'top-down' blocking strategy to create a structured mesh. The 'tetra' mesh was achieved using a 'bottom-up' meshing method by creating a surface mesh which was then refined to produce a finer volume mesh. 'Hexa' meshing was favoured over 'tetra' meshing as less computational points are needed, a higher spatial resolution is observed and the mesh has a better aspect ratio [19]. However, this method is not always realistic with complex geometries. 'Hexa' meshing was used in sections 2 and 3, as for the 'free surface' model it was important to have an increased mesh resolution around the air-water interface to accurately capture the interface motion and enhance the results. A 'tetra' mesh was used in section 1 due to the complex nature of the turbine geometry, however, problems using tetrahedral cells in the boundary layer are well known [20], so prism layers were added to the surface of the turbine to help increase the boundary layer resolution perpendicular to the wall. Further information about these meshing techniques can be found in [21].

A mesh study was carried out on section 1 to ensure that mesh refinement around the turbine was to an acceptable level while taking into consideration computational time and model accuracy. The mesh in sections 2 and 3 remained constant. 7 different meshes were generated and run with the conditions specified in Table III. This study was carried out using the 'free surface' model as the same mesh would be used for both the 'free surface' and 'free slip' models to allow direct comparison between the simulations. Tests were carried out for a single angular velocity at peak power (TSR = 4).

The maximum mesh sizing on the blades and the hub was investigated as well as the mesh distribution over the blade root, middle and tip. The effect of prism layers perpendicular to the turbine surfaces were also considered with various number of layers and first layer thickness investigated.

C) Physics setup

All numerical modelling was carried out using ANSYS CFX 18.0 [22] as a transient analysis to capture the time dependent nature of the flow and the dynamic loading on the turbine. A cylinder surrounding the turbine was used to employ the MFR technique, allowing the 'turbine' domain to move relative to the stationary 'flume' domain, simulating the turbine rotation. A 'transient rotor stator' interface model was used to account for the transient interaction effects at the sliding interface between the 2 domains. This rotation was controlled using the angular velocities (ω) found by experimental testing. These angular velocities, along with their approximate corresponding Tip Speed Ratios (TSR), are described in Table V. The TSR (λ) is the ratio between the blade tip velocity (ωR), and the water velocity ($\bar{W}$), as shown by (1):

$$\lambda = \frac{\omega R}{\bar{W}} \tag{1}$$

The 'free slip' model was treated as single phase, incompressible flow while the 'free surface' simulation used a homogenous multiphase model, incorporating

TABLE III.
A SUMMARY OF EACH MESH SETUP.

Mesh Number	Element size on each part (m)					Prism Layer Properties			Total Elements (millions)	
	MFR Cylinder	Blade Tip	Blade Middle	Blade Root	Hub	First layer thickness (m)	No. Layers	Growth Rate	MFR cylinder	Whole domain
1	0.024	0.003	0.005	0.007	0.008	0.002	3	1.0	2.89	6.92
2	0.024	0.003	0.005	0.007	0.008	0.001	3	1.0	2.96	6.99
3	0.024	0.005	0.008	0.011	0.012	0.001	3	1.0	1.47	5.53
4	0.024	0.002	0.004	0.005	0.006	0.001	3	1.0	4.67	8.64
5	0.024	0.003	0.005	0.007	0.008	0.0005	3	1.0	3.03	7.06
6	0.024	0.002	0.004	0.004	0.006	0.00075	6	1.0	3.1	7.08
7	0.024	0.002	0.004	0.004	0.006	-	0	-	2.9	6.94

TABLE V.
ANGULAR VELOCITIES USED TO CONTROL TURBINE ROTATION.

Angular Velocity, ω (rad/s)	Approximate TSR, λ
0.0	0
2.2215	1
4.4435	2
6.6652	3
8.8878	4
11.1088	5
13.3313	6
15.5529	7

buoyancy effects, with 2 fluid phases separated by a distinct interface. Volume fractions were used to specify the quantities of each phase at the inlet with (2) giving the volume fractions of each fluid:

$$V_1 = r_1 V \tag{2}$$

Where r_1 is the volume fraction of fluid 1, and V_1 is the volume occupied by fluid 1 in an overall volume, V [23]. The volume fraction advection scheme, for free surface flows, is controlled by interface compression [24]. This in turn controls the interface sharpness and is set at a setting of 2 for 'aggressive compression'.

The Shear Stress Transport (SST) turbulence model was used to close the Reynolds Averaged Navier Stokes (RANS) equations in order to resolve the flow conditions. This is a 2-equation turbulence model combining the k-ω and k-ε turbulence models. ANSYS CFX uses an 'automatic near-wall treatment' for ω-based turbulence models which allows automatic switching from the low-Re near wall formulation, to wall functions based on the refinement of the mesh [25]. The SST turbulence model has specifically been used in this application due to improved performance under adverse pressure gradients and for accurate boundary layer simulations necessary in general turbine modelling [26].

For both the 'free surface' and 'free slip' models, the boundary conditions for the inlet were set as a 'velocity-inlet' with a streamwise water velocity of 1.01 m/s, taken from the average experimental velocity. Figure 5 shows the boundary conditions used in each model setup. Both the models had the outlet set as a 'pressure-outlet', with the 'free slip' model using a relative pressure of 0 Pa, and the 'free surface' model using 0 Pa in the 'air' region and a hydrostatic pressure in the 'water' region. The two side

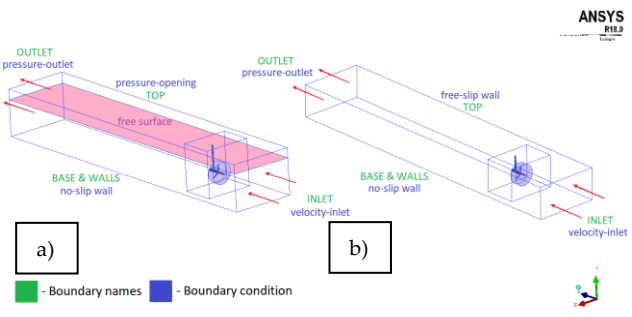

Figure 5. Boundary conditions imposed for: (a) 'free surface' and; (b) 'free slip' models.

TABLE IV.
BOUNDARY CONDITION DETAILS.

Boundary	Boundary Condition	
	'free surface' model	'free slip' model
inlet	Velocity-inlet $\bar{W} = 1.01\ m/s$	Velocity-inlet $\bar{W} = 1.01\ m/s$
outlet	Pressure-outlet $P_{ref} = (\rho_{water} - \rho_{air}) \cdot g \cdot (h - y)$	Pressure-outlet $P_{ref} = 0\ Pa$
top	Pressure-opening Entrainment with opening pressure: $P_{rel} = 0\ Pa$	Free-slip wall
base	No-slip wall	No-slip wall
walls	No-slip wall	No-slip wall

walls along with the base of the tank were specified as 'no-slip walls' to incorporate the effect of friction near the tank walls. The stanchion, hub and blades of the turbine were also 'no-slip walls' for both models. The main difference between the setup of the models were the boundary conditions used to represent the 'top' boundary. The 'free slip' model used a 'free-slip wall' boundary condition which defined the velocity component parallel to the wall as a finite value while normal to the wall was zero [23]. The 'free surface' model used an 'opening' to represent the 'top' boundary which allows flow into and out of the boundary, being less restrictive and allowing movement over the water surface. A summary of the boundary conditions used in both models are shown in Table IV.

The time step for each simulation was defined by the angle (θ) through which the turbine turned per time step (Δt). A time step was chosen to equal the time taken for the turbine to rotate by θ = 5° which agreed with the findings of [9] and the recommendation by [27]. The angular frequency of the turbine would change depending on the desired TSR, and therefore the time step for each model would be varied accordingly.

All simulations reached convergence after 40 seconds of run time and therefore all results reported in this study were taken after this time in a period of solution stability. Monitor points in the upstream of the domain were added to observe changes through the water depth in the velocity over time. The torque and thrust, on each of the blades and the hub, were monitored every time step to examine the transient loading at different angular velocities, as well as to monitor the convergence of the simulation. This was implemented using expressions created with CFX Expression Language (CEL) as shown in (3):

$$Torque\_z\_Rot\ Axis()@Blade1 \tag{3}$$

Where '$Torque$' is the function being carried out, '$\_z$' specifies the rotational axis with '$\_Rot\ Axis$' being the name of the local coordinate frame, and '$Blade1$' referring to the turbine surface used.

All simulations used 'Double Precision' when defining the run as this setting permits more accurate numerical mathematical operations and improves convergence which is necessary in multiphase modelling [24]. These simulations were carried out using the High Performance

Computing (HPC) cluster, 'Hawk', through access from Cardiff University. All models were run using 40 processors over 1 node. For 'free surface' modelling, it was important to restrict the partitioning direction used so that the free surface was not aligned with any partition boundaries when running in parallel. This can cause problems with running the simulation and therefore partitioning was restricted to the x and z directions only, and not in the y direction.

IV. Results and Discussion

A) *Mesh independence study*

A number of meshes, as detailed in Table III, were generated in order to investigate the effects of mesh refinement on the performance characteristics of the turbine. The maximum mesh size and distribution on the blades and hub was investigated. The torque (Q) and thrust (F), on the hub and on each blade, were monitored to calculate the non-dimensional power (C_p), thrust (C_t) and torque (C_q) coefficients. These are defined as shown in (4) - (6) where the swept area, $A = \pi(R^2)$:

$$C_p = \frac{P_{output}}{P_{available}} = \frac{Q\omega}{\frac{1}{2}\rho A W^3} \tag{4}$$

$$C_t = \frac{F_{output}}{F_{available}} = \frac{F_{output}}{\frac{1}{2}\rho A W^2} \tag{5}$$

$$C_q = \frac{Q_{total}}{F_{available} \cdot R} = \frac{Q_{total}}{\frac{1}{2}\rho A W^2 \cdot R} \tag{6}$$

These coefficients were used to compare each numerical model result to the experimental data as shown in Figure 6. These comparisons helped to guide the development of the turbine mesh, as well as results and methods reported by [9], [28], [29].

Mesh 1 was developed as the 'base' mesh, upon which other arrangements were established. Each mesh ranged from having ≈1.5 – 4.7 million elements in the MFR cylinder resulting in ≈5.8 – 9.0 million elements in total. It was found that inflation layers on the turbine surface were necessary as without them, C_p, C_t and C_q were all overpredicted as shown by mesh 7 in Figure 6. Overall, it was found that mesh 6 gave the best agreement to experimental results at a TSR of 4. The C_p and C_q differed from the experimental data by < 3%, while the difference between the data sets for C_t was 12%. Results for C_p and C_q were both within 1 standard deviation of the experimental data while agreement for C_t was not as good, however, all meshes experienced the same discrepancies in C_t. It was recommended by [24] to have a mesh with at least 10 nodes in the boundary layer region for accurate representation of these flow effects. This gives a $y^+ < 2$ which is found to be excessive and is hard to satisfy for all wall regions. Due to the considerable increase in the number of elements needed to satisfy $y^+ < 2$, this numerical testing used $y^+ = 65 – 220$, dependent on the TSR, which was found to be acceptable as discussed by [29], [30]. The focus of this study was to compare the differences between the results in a 'free surface' and a 'free slip' model. Therefore, exact agreement with experimental results, over the whole range of TSR's, was not vital and hence mesh 6 gave a good degree of accuracy for this work. The final overall mesh can be seen in Figure 7.

B) *Numerical validation using experimental data*

To enable a comparison between the 2 types of numerical model, it was initially important to validate the models using experimental data. Figure 8 shows the

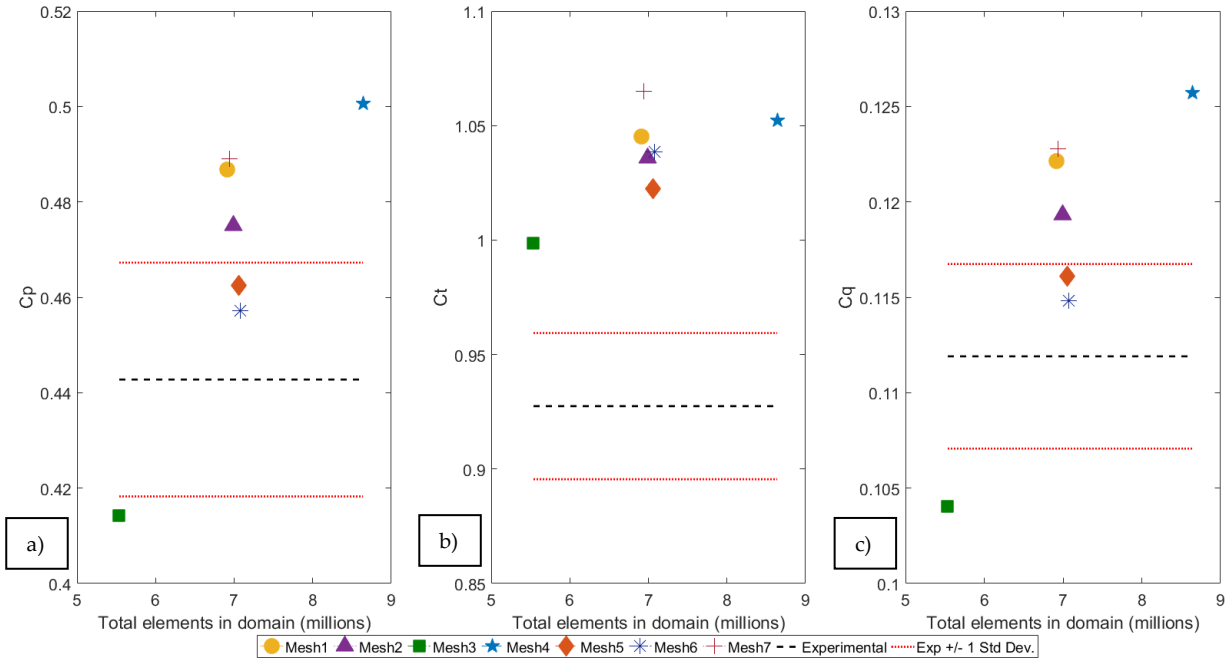

Figure 6. Mesh comparison between numerical and experimental results for: (a) Cp, (b) Ct and; (c) Cq.

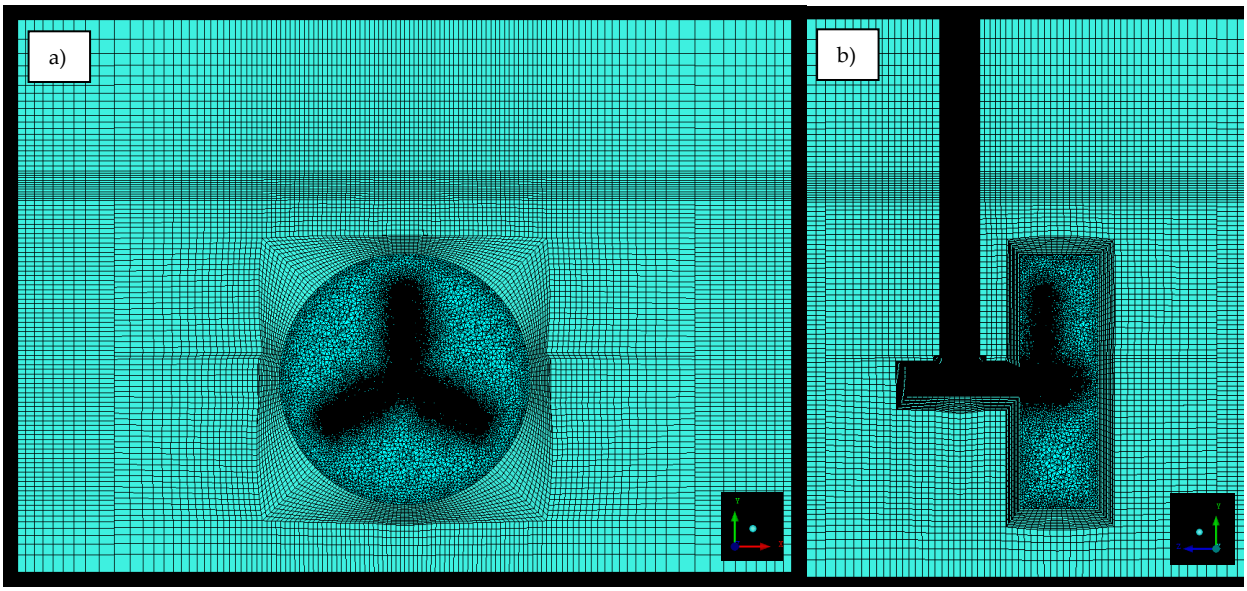

Figure 7. Final overall mesh for section 1-3 in the 'free surface' model.

average values of C_p and C_t over a range of TSR values for the numerical and experimental data, with the error bars on the experimental data showing +/- 1 standard deviation. Initially looking at Figure 8a, the numerical C_p showed good agreement with the experimental data for TSR values up to 5, with differences of < 0.04 present between the data sets. At higher TSR values, the CFD results dropped off a lot quicker than the equivalent experimental values, with differences in C_p of up to 0.3.

A similar trend can be seen for values of C_t in Figure 8b, with a bigger divergence occurring after a TSR of 4, but instead with the CFD overpredicting the higher TSR values. Below a TSR of 4, the difference between the numerical and experimental C_t was < 0.06. This increased to a difference of 0.11 for TSR values of 5-7.

One possible reason for these observations could be due to inaccuracies in modelling the boundary layer. As the angular velocity increases at higher TSR values, the flow conditions become more complex and therefore it is possible that flow separation was occurring in a less refined part of the mesh due to the angle of attack changing with the angular velocity. For the purpose of this study, a comparison between the model types at a TSR of 3-5 was investigated as this was the region of peak power that was of interest and gave the best agreement with the experimental data.

C) 'Free surface' and 'free slip' model comparison

To identify the differences in the results produced by the 'free surface' and the 'free slip' models, the same inlet velocity and range of rotational turbine velocities were tested, as in the experimental data set. These angular velocities corresponded to a TSR of between 0 and 7 while the inlet velocity was set to 1.01 m/s. Comparisons were made between the 2 types of model, with a focus on the average and transient dynamic loadings.

Figure 9 shows the thrust and torque values obtained on each blade for 5s of converged run time for both the 'free surface' and the 'free slip' numerical models at a TSR of 3-5. It was clear to see that the rotational period for both types of model were as expected, giving 0.94s, 0.71s and

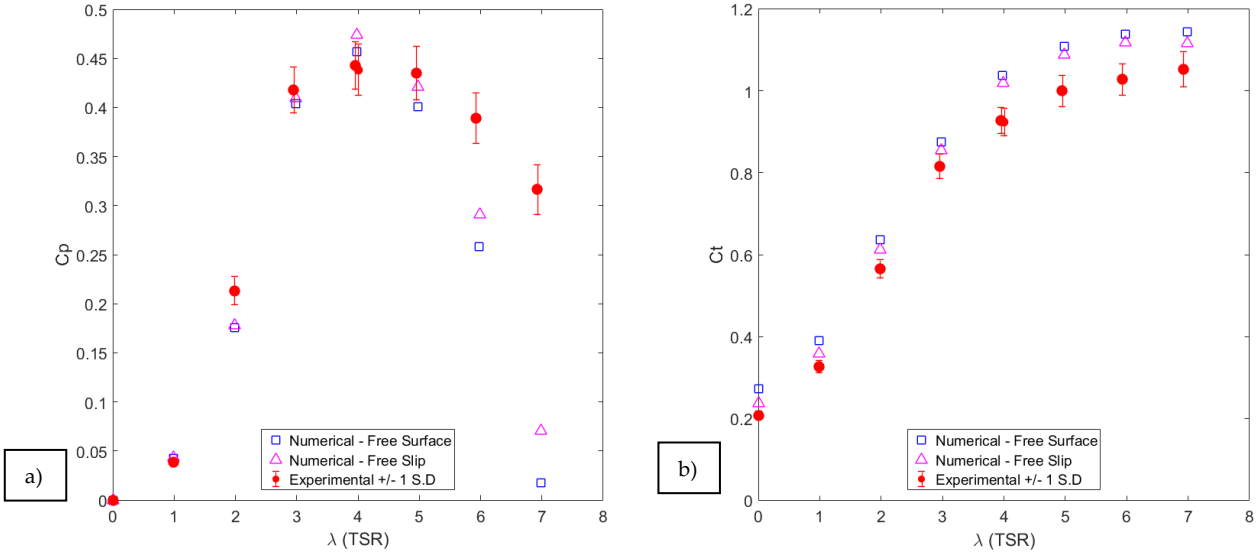

Figure 8. Comparisons between the numerical model results and experimental data for: (a) Cp and; (b) Ct.

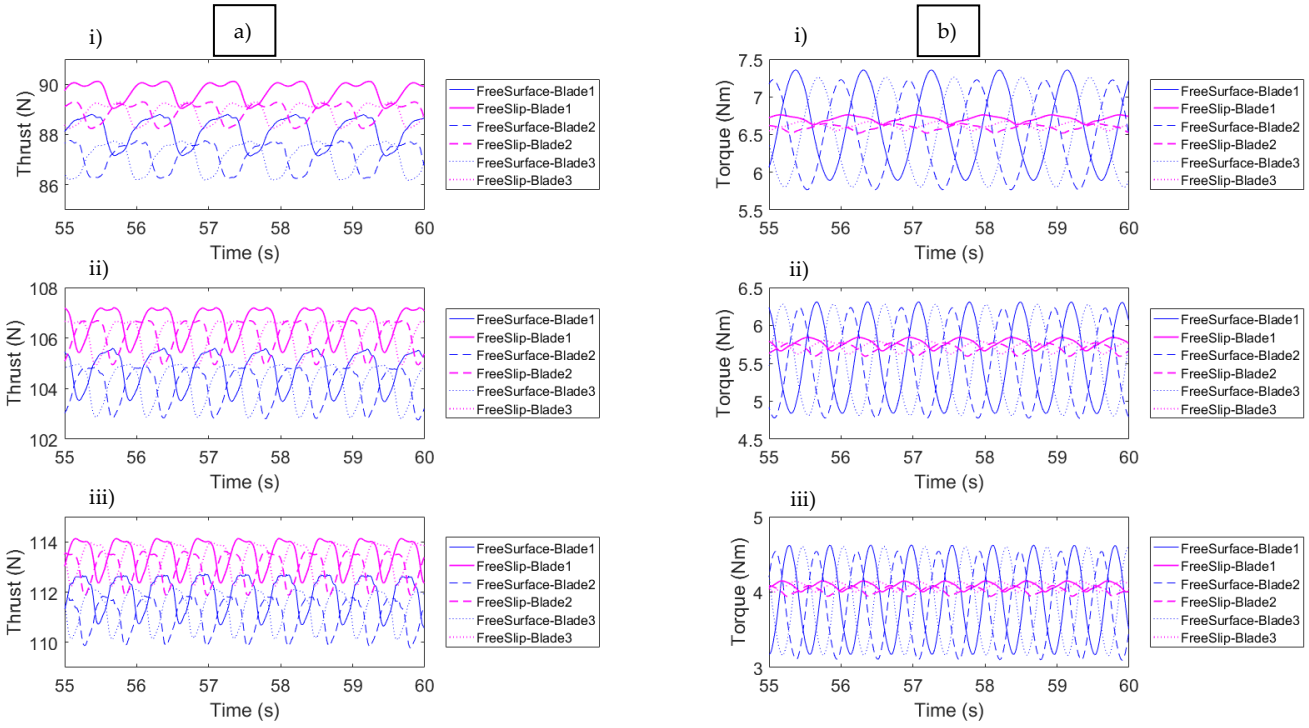

Figure 9. Numerical comparison between the 'free surface' and 'free slip' models, for (a) thrust and (b) torque results on each blade over 5s of converged tun time for: (i) TSR 3, (ii) TSR 4 and; (iii) TSR 5.

0.57s for TSR 3, 4 and 5 respectively. The clear drop in thrust every period was due to a single blade passing the stanchion each rotation and was identical to the rotational frequency of the turbine.

The difference in average thrust for each blade at TSR 3-5 was on average 1.8 N greater for the 'free slip' models in comparison to the 'free surface' models. The 'free slip' models also had an average torque for each blade of 0.16 Nm greater than the 'free surface' models. For both thrust and torque, the 'free slip' models gave higher average predictions for each blade, however, these differences were very small and were not significant. This observation can be seen more clearly in Figure 10 (i) which displays the comparison between the 'free surface' and 'free slip' models, for the thrust and torque measured at a TSR of 4 on different sections of the turbine over time. As for a single turbine blade, the average torque on the hub showed little difference between the 2 types of model, as shown in Figure 10b(ii). The difference in average thrust on the hub, however, showed a much greater contrast between the 2 types of model (Figure 10a(ii)). The 'free surface' model predicted an average thrust of 20.1 N while the 'free slip' model estimated 8.2 N. This was a significant difference as the thrust on the hub of the 'free surface'

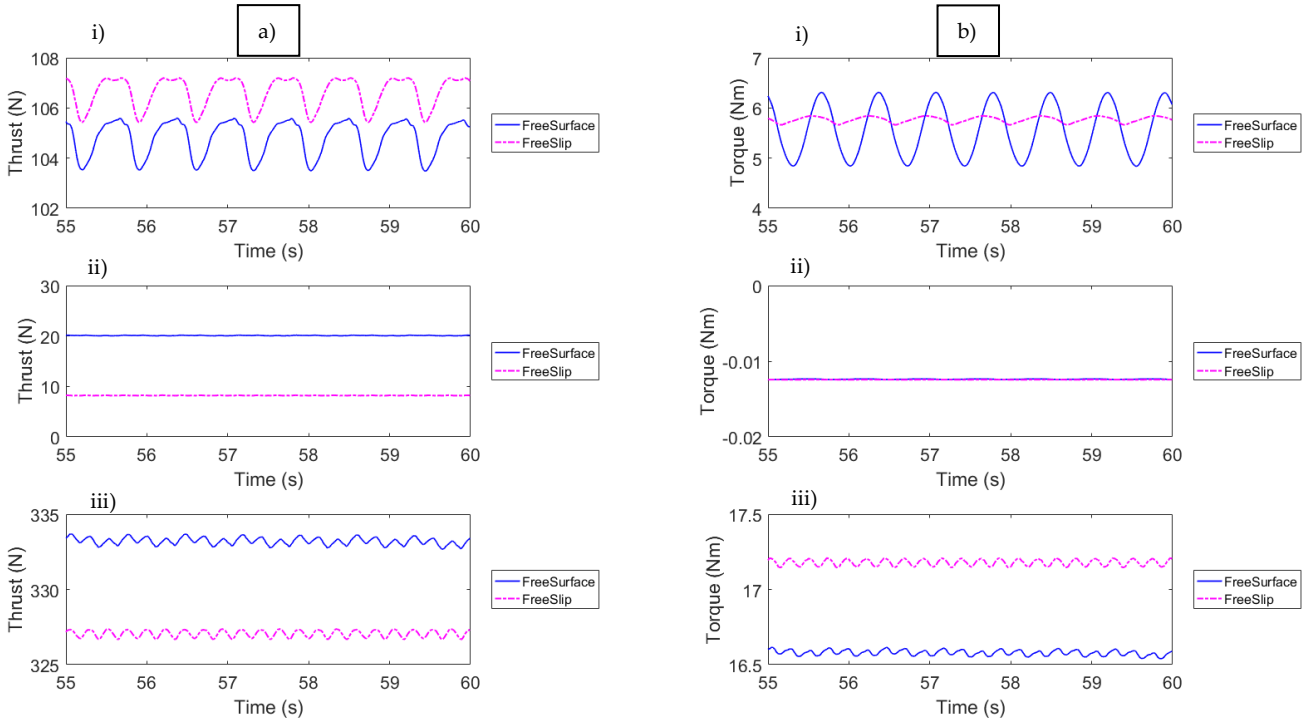

Figure 10. Numerical comparison between the 'free surface' and 'free slip' models, for (a) thrust and (b) torque results at TSR 4 relating to: (i) blade 1, (ii) the hub and; (iii) the turbine total (all blades and hub).

model was over double that of the 'free slip' model. This was because the 'free slip' model neglected the hydrostatic and atmospheric pressure unlike the 'free surface' model. This resulted in a difference between the model predictions for the hub forces as the contribution of the hydrostatic forces was significant at this location. Consequently, Figure 10a(iii) shows that the 'free surface' model estimated a higher overall average thrust of 6.2 N greater than the 'free slip' model, which was primarily down to the significant difference in the hub predictions of each model. This resulted in the prediction for C_t being lower than expected and gives the false impression that the 'free slip' estimation of C_t had better agreement to the experimental values in comparison to the 'free surface' model. Instead, it was just failing to account for certain components of the overall force. The overall average torque results, however, were as expected with the 'free slip' model estimating a marginal 0.6 Nm greater than the 'free surface' model.

The significant differences in the thrust results for the hub were not seen in the blade thrust results. This was because the hub was static in the water depth where the hydrostatic pressure gave the main contribution to the hub forces. In comparison, the blades were moving and therefore the dynamic pressure in the stream wise direction was dominating here.

The shape of the transient thrust results for each individual blade showed very good agreement between the 2 types of model. However, there were some slight discrepancies between the average thrust for blade 1 in comparison to blades 2 and 3. This observation occurred in both numerical models where the average thrust results for blades 1, 2 and 3 varied by a maximum difference of 1 N. This had little effect on the overall thrust, but it should still be noted as it was expected that all blades 1-3 would have the same average thrust. It was therefore hypothesised that the mesh on each blade was marginally different as the 'tetra' mesh around the turbine was automatically generated and so it cannot be guaranteed that each blade mesh was identical, accounting for the small difference in results. The shape of the transient torque results was much more contrasting as the amplitude of the fluctuation for each type of model was very different.

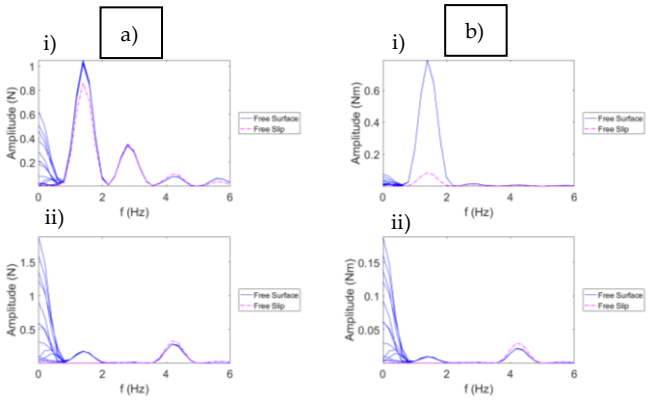

Figure 11. 'Free surface' model FFT for the (a) thrust and (b) torque at TSR 4 for: (i) blade 1 and; (ii) the turbine total (all blades and hub).

A Fast Fourier Transform (FFT) was carried out to examine the magnitude of the fluctuation in the data sets. Figure 11 shows the FFT spectra produced by the 'free surface' and 'free slip' models for the thrust and torque results at a TSR of 4, for a single blade as well as the combined turbine totals. Figure 11(i) clearly shows there is a dominant peak for blade 1 at a frequency of 1.41 Hz which corresponds to the frequency of the blade crossing the stanchion each rotation. In Figure 11(ii), the dominant frequency is smaller and at 4.24 Hz, which corresponds with each blade crossing the stanchion and occurs 3 times per rotation.

It was found that for the full range of TSR values, 1-7, the fluctuation in the thrust measurements for a single blade was higher for the 'free surface' models with an average amplitude of 0.95 +/- 0.067 N compared to the 'free slip' models with 0.75 +/- 0.137 N. This shows that the magnitude of fluctuation for a single blade remained constant across all angular velocities and showed only minor differences between the amplitude of thrust fluctuation for each model type. This can be seen by looking at the FFT in Figure 11a(i) or the transient thrust results in Figure 10a(i). The same trend was apparent in the amplitude of fluctuation for the hub and the total thrust results, even though the average values were very different.

In comparison, the fluctuation in the torque results had a much bigger contrast with the 'free surface' models showing considerably greater fluctuations, following the same trend as TSR 4 shown in Figure 11b(i) and Figure 10b(i). The amplitude of the torque fluctuation for all TSR values was 0.77 +/- 0.012 Nm for the 'free surface' model while the 'free slip' model averaged 0.06 +/- 0.017 Nm. This represents a significant difference between the 2 model predictions. A possible explanation for this is, again, the difference between the total pressures in each model. Buoyancy forces act in the vertical direction only and so when the position of a blade is at top dead centre or bottom dead centre, these buoyancy forces do not contribute to the torque on the blade. However, when the blade is half way between these positions, the buoyancy force will have a much greater contribution to the torque on the blade resulting in the oscillations seen in the transient torque results. The 'free slip' torque results have neglected these buoyancy forces and therefore all that is being seen here is the dynamic pressure term used to predict the torque around the global axis of rotation.

Even though the amplitude of torque fluctuation for a single blade showed these observations, the total torque fluctuation showed no difference between the 'free surface' and 'free slip' models. This was because the blades were 120° out of phase and so, as shown in Figure 11, each blade cancelled the others out and reduced the amplitude of the frequency. This emphasises the fact that if only the overall thrust and torque were analysed, fundamental characteristics would be overlooked from the individual blade and hub loadings. This could be vital for fatigue and

survivability analysis. However, in practice a local velocity profile or other complex flow conditions would result in local variation in the velocity masking those previously stated. Yet, it is still important to analyse the individual component loadings as with more complex conditions and bigger fluctuations these effects will only be enhanced.

V. CONCLUSION

A 3D numerical comparison has been carried out to analyse the differences in flow conditions and turbine performance with 2 different surface boundary conditions. A 'free surface' and a 'free slip' model were developed to replicate testing of a 0.9m diameter turbine at the IFREMER flume facility. The thrust and torque of the turbine was measured in a transient analysis at angular velocities corresponding to a TSR of 0-7.

A mesh study was carried out to ensure the grid refinement was to an acceptable level. Mesh 6 was found to have best agreement with experimental results, giving a difference of < 3% for C_p and C_q, and 12% for $C_t$at TSR 4. This provided a sufficient level of accuracy for this work as the focus of this study was to compare the differences between the 'free surface' and 'free slip' model set up.

Minor differences were observed between the average thrust and torque on an individual blade as well as the total average thrust and torque over the whole turbine. The fundamental differences between the 2 models were the predictions in average thrust on the hub, and the fluctuation in the transient results for the torque over an individual blade. The 'free surface' model estimated an average thrust on the hub of over twice that of the 'free slip' model, showing a significant difference. Similarly, the fluctuation in the torque results over an individual blade was much greater in the 'free surface' model.

Overall, the difference between the models in average values for thrust and torque on each turbine blade were not significant. Therefore, if this is of interest, either model would be adequate. To get an accurate measure of the thrust on the hub, it would be necessary to use the 'free surface' model. Similarly, if the transient loadings were important the 'free surface' model should be used as it gave a better representation of the higher levels of fluctuation as expected in real flow conditions.

ACKNOWLEDGEMENTS

This research used the supercomputing facilities at Cardiff University operated by Advanced Research Computing at Cardiff (ARCCA) on behalf of the Cardiff Supercomputing Facility and the HPC Wales and Supercomputing Wales (SCW) projects. We acknowledge the support of the latter, which is part-funded by the European Regional Development Fund (ERDF) via the Welsh Government. The experimental testing was funded by EPSRC Impact Acceleration Account funding and supported by IFREMER.

REFERENCES

[1] European Commission, *Strategic Energy Technology Plan*. 2017.
[2] Ocean Energy Europe, "Ocean energy project spotlight: Investing in tidal and wave energy," 2017.
[3] M. Harrison, W. Batten, L. Myers, and A. Bahaj, "Comparison between CFD simulations and experiments for predicting the far wake of horizontal axis tidal turbines," *IET Renew. Power Gener.*, vol. 4, no. 6, pp. 613–627, 2010.
[4] M. J. Churchfield, Y. Li, and P. J. Moriarty, "A large-eddy simulation study of wake propagation and power production in an array of tidal-current turbines," *Philos. Trans. R. Soc.*, 2013.
[5] A. C. W. Creech, A. G. L. Borthwick, and D. Ingram, "Effects of support structures in an LES actuator line model of a tidal turbine with contra-rotating rotors," *Energies*, vol. 10, no. 5, 2017.
[6] X. Li *et al.*, "Modelling impacts of tidal stream turbines on surface waves," *Renew. Energy*, vol. 130, pp. 725–734, Jan. 2019.
[7] T. O'Doherty, A. Mason-Jones, D. M. O'Doherty, C. B. Byrne, I. Owen, and Y. X. Wang, "Experimental and Computational Analysis of a Model Horizontal Axis Tidal Turbine," in *Proceedings of the 8th European Wave and Tidal Energy Conference, Uppsala, Sweden*, 2009.
[8] C. Frost, C. E. Morris, A. Mason-Jones, D. M. O'Doherty, and T. O'Doherty, "The effect of tidal flow directionality on tidal turbine performance characteristics," *Renew. Energy*, vol. 78, pp. 609–620, 2015.
[9] R. McSherry, J. Grimwade, I. Jones, S. Mathias, A. Wells, and A. Mateus, "3D CFD modelling of tidal turbine performance with validation against laboratory experiments," *EWTEC 2011 Proc.*, 2011.
[10] J. Yan, X. Deng, A. Korobenko, and Y. Bazilevs, "Free-surface flow modeling and simulation of horizontal-axis tidal-stream turbines," *Comput. Fluids*, vol. 158, pp. 157–166, Nov. 2017.
[11] T. G. Thomas and J. J. R. Williams, "Development of a parallel code to simulate skewed flow over a bluff body," *J. Wind Eng. Ind. Aerodyn.*, pp. 155–167, 1997.
[12] X. Bai, E. J. Avital, A. Munjiza, and J. J. R. Williams, "Numerical simulation of a marine current turbine in free surface flow," *Renew. Energy*, vol. 63, pp. 715–723, 2014.
[13] X. Sun, J. P. Chick, and I. G. Bryden, "Laboratory-scale simulation of energy extraction from tidal currents," *Renew. Energy*, vol. 33, pp. 1267–1274, 2008.
[14] R. Ellis *et al.*, "Design Process for a Scale Horizontal Axis Tidal Turbine Blade .," *Proc. 4th Asian Wave Tidal Energy Conf.*, 2018.
[15] M. Allmark, R. Ellis, K. Porter, T. O. Doherty, and C. Johnstone, "The Development and Testing of a Lab-Scale Tidal Stream Turbine for the Study of Dynamic Device Loading," *Proc. 4th Asian Wave Tidal Energy Conf.*, 2018.
[16] B. Gaurier, P. Davies, A. Deuff, and G. Germain, "Flume tank characterization of marine current turbine blade behaviour under current and wave loading," vol. 59, pp. 1–12, 2013.
[17] R. Howell, N. Qin, J. Edwards, and N. Durrani, "Wind tunnel and numerical study of a small vertical axis wind turbine," *Renew. Energy*, vol. 35, pp. 412–422, 2009.
[18] ANSYS Inc, "ANSYS ICEM." Release 18.0.
[19] A. Raval, "Numerical Simulation of Water Waves using Navier-Stokes Equations," PhD Thesis, University of Leeds, 2008.
[20] M. O. L. Hansen, J. N. Sørensen, S. Voutsinas, N. Sørensen, and H. A. Madsen, "State of the art in wind turbine aerodynamics and aeroelasticity," *Prog. Aerosp. Sci.*, vol. 42, pp. 285–330, 2006.
[21] ANSYS Inc, "ANSYS ICEM Help Manual." Release 18.0.
[22] ANSYS Inc, "ANSYS CFX." Release 18.0.
[23] ANSYS Inc, "ANSYS CFX Theory Guide." Release 18.0.
[24] ANSYS Inc, "ANSYS CFX Modelling Guide." Release 18.0.
[25] F. Menter, M. Kuntz, and R. Langtry, "Ten Years of Industrial Experience with the SST Turbulence Model," in *Proceedings of the 4th International Symposium on Turbulence, Heat and Mass Transfer*, 2003.
[26] ANSYS Inc, "Innovative Turbulence Modeling: SST Model in ANSYS CFX," 2004.
[27] ANSYS Inc, "ANSYS CFX Reference Guide." Release 18.0.
[28] T. O'Doherty, A. Mason-Jones, D. O'Doherty, P. Evans, C. Wooldridge, and I. Fryett, "Considerations of a horizontal axis tidal turbine," *Proc. Inst. Civ. Eng. - Energy*, vol. 163, no. EN3, 2010.
[29] C. Frost, "Flow Direction Effects On Tidal Stream Turbines," PhD Thesis, Cardiff University, 2016.
[30] A. Mason-Jones, "Performance assessment of a Horizontal Axis Tidal Turbine in a high velocity shear environment," PhD Thesis, Cardiff University, 2009.